Three-Dimensional Numerical Studies of the Temperature Anisotropy Instability in Intense Charged Particle Beams*

Edward Startsev, Ronald C. Davidson and Hong Qin
Plasma Physics Laboratory, Princeton University
Princeton, NJ, USA

2004 International Symposium on Heavy Ion Inertial Fusion
June 7-11, 2004

*Research supported by the U.S. Department of Energy.

Abstract

- In neutral plasmas with a uniform magnetic field and strongly anisotropic distribution function ($T_{||}/T_{\perp} \ll 1$) an electrostatic Harris-type collective instability may develop if the plasma is sufficiently dense.

- Such anisotropies develop naturally in accelerators, and a similar instability may lead to a detoriation of the beam quality in a one-component nonneutral charged particle beam.

- The instability may also lead to an increase in the longitudinal velocity spread, which would make the focusing of the beam difficult and impose a limit on the minimum spot size achievable in heavy ion fusion experiments.

- This paper reports the results of recent numerical studies of the temperature anisotropy instability using the newly developed Beam Eigenmode And Spectra (bEASt) code for space-charge-dominated, low-emittance beams with large tine depression ($\nu/\nu_0 \ll 1$).

- Such high-intensity beams are relevant to next-step experiments such as the Integrated Beam Experiment (IBX), which would serve as proof-of-principal experiment for heavy ion fusion.

Spot size requirements

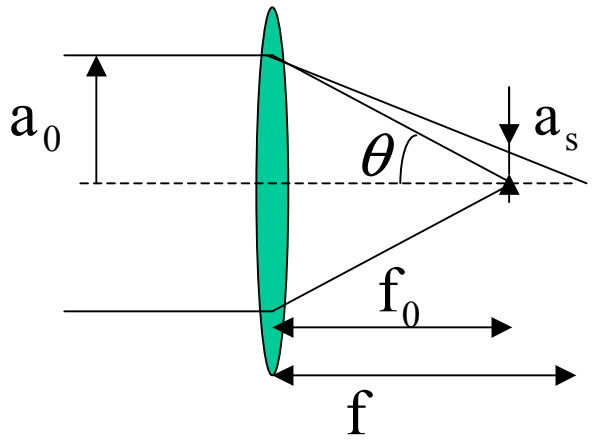

$$a_s \approx \theta \left| f - f_0 \right| \quad \text{spot size}$$

$$f = f_0 (1 + \Delta v_z / v_z) \qquad a_s \approx (2-8) a_0 \left| \Delta v_z / v_z \right|$$

Need to have beam with

$$\left| \Delta v_z / v_z \right| \leq 1\%$$

Harris instability in eclectically neutral plasma with uniform magnetic field

- Anisotropic electron distribution ($T_{||b}/T_{\perp b} < 1/2$) is required.

- Plasma must be sufficiently dense that $\omega_{pe} > \omega_{ce}$, where $\omega_{pe} = (4\pi e^2 n/m)^{1/2}$ is the electron plasma frequency and $\omega_{ce} = eB/mc$ is the electron cyclotron frequency.

- Instability is very fast $\gamma \sim \omega_{pe}$.

*E. G. Harris, Phys. Rev. Lett. **2**, 34 (1959).

Harris Instability in Intense One-Component Beams

- For the case of charged particle beams in accelerators the cyclotron oscillations in the applied magnetic field are replaced by the betatron oscillations of the beam particles in the combined applied and self-generated fields.

$$\omega_{ce} \longrightarrow \omega_{\beta b}.$$

- Heavy ion fusion experiments require transporting high-current beams when the average depressed betatron frequency of the beam particles is much smaller then the average plasma frequency of the beam particles.

$$\omega_{\beta b} \ll \omega_{pb}.$$

Temperature anisotropies ($T_{||b} << T_{\perp b}$) develop neutrally in accelerators

- For particles with charge e_b and mass m_b accelerated by a voltage V, the energy spread of particles in the beam does not change, and (nonrelativistically)

$$\Delta E_{bi} = m_b \Delta v_{bi}^2/2 = \Delta E_{bf} = m_b V_b \Delta v_{bf},$$

  where $V_b = (e_b V/m_b)^{1/2}$ is the average beam velocity after acceleration.

- Therefore, the velocity spread-squared, or equivalently the temperature, changes according to (for a nonrelativistic beam)

$$T_{||bf} = T_{||bi}^2/2e_b V.$$

- For example for $T_{||i} = 1eV$, $e_b V = 1MeV$, $T_{||f} = 5 \times 10^{-7} eV$

Previous Studies of Temperature anisotropy instability in Intense One-Component Beams

- Analytical theory by Wang and Smith (1982) for axisymmetric perturbations about the beam with a Kapchinskij − Vladimirskij (KV) distribution assuming infinite anisotropy with $T_{||b}/T_{\perp b} = 0$.

- 3D PIC simulations by Friedman, et. al.(1990) using the WARP code observed a rapid temperature 'equilibration' process of KV beams with large temperature anisotropy.

- WARP simulations by Lund, et. al.(1998) using a semi-gaussian distribution to avoid the numerous unstable modes introduced by the KV distribution.

- Shortcomings:
  - WARP is sufficiently noisy that resolving the linear stage of instability with sufficient accuracy is very difficult.
  - KV distribution has a highly unphysical (inverted) population in transverse phase-space variables.
  - Semi-gaussian distribution is not a rigorous equilibrium solution ($\partial/\partial t = 0$) of the Vlasov-Maxwell equations about which to perturb.

Instability Mechanism

- KV distribution as an example.

- Dipole mode has the highest growth rate.

$$\delta\phi(\mathbf{x},t) = \hat{\phi}\frac{x}{r_b}\exp(ik_z z - i\omega t)$$

- Growth rate is an increasing function of $k_z r_b$ and approaches its limiting value for $k_z^2 r_b^2 \gg 1$. Therefore, $k_z^2 r_b^2 \gg 1$ is assumed and $\delta\mathbf{E} \simeq -ik_z\delta\phi\mathbf{e}_z$.

- Use equivalent KV beam where all of the particles oscillate with the same frequency, equal to the average depressed betatron frequency $\omega_{\beta\perp} = 2T_{\perp b}/m_b r_b^2$

$$x(t) = \hat{x}\cos(\omega_{\beta\perp}t + \alpha_0)$$

where α_0 is the oscillation phase at $t = 0$ and $\hat{x} = \sqrt{2H_x/m_b}/\omega_{\beta\perp}$ is the oscillation amplitude.

Instability Mechanism

- Longitudinal equation of motion for a beam particle becomes

$$\ddot{z} = -ik_z \frac{e_b}{m_b} \hat{\phi} \frac{\hat{x}}{r_b} \cos(\omega_{\beta\perp} t + \alpha_0) e^{ik_z z_0 - i\omega t}$$

- Integrating with respect to time, we obtain

$$z_\alpha = ik_z \frac{e_b}{m_b} \hat{\phi} \frac{\hat{x}}{2r_b} \left[\frac{e^{i\alpha}}{(\omega - \omega_{\beta\perp})^2} + \frac{e^{-i\alpha}}{(\omega + \omega_{\beta\perp})^2} \right] e^{ik_z z_0 - i\omega t},$$

  where $\alpha = \alpha_0 + \omega_{\beta\perp} t$.

- Note that the individual particle motion has two characteristic frequencies, $\omega - \omega_{\beta\perp}$ and $\omega + \omega_{\beta\perp}$.

Instability Mechanism (Dispersion relation)

- Average displacement $\langle z\rangle(x,z,t) = (z_\alpha + z_{-\alpha})/2$ is

$$\langle z\rangle(x,z,t) = ik_z \frac{e_b}{m_b}\hat{\phi}\frac{x}{2r_b}\left[\frac{1}{(\omega-\omega_{\beta\perp})^2}+\frac{1}{(\omega+\omega_{\beta\perp})^2}\right]e^{ik_z z - i\omega t},$$

- or, since $\delta E_z = -ik_z\delta\phi$,

$$\langle z\rangle(x,z,t) = -\frac{e_b\delta E_z}{2m_b}\left[\frac{1}{(\omega-\omega_{\beta\perp})^2}+\frac{1}{(\omega+\omega_{\beta\perp})^2}\right].$$

- From the continuity equation for the density perturbation,

$$\frac{\partial\delta n}{\partial t}+\frac{\partial}{\partial z}\left(n_0\frac{\partial\langle z\rangle}{\partial t}\right)=0, \quad \Rightarrow \quad \delta n = -n_0\frac{\partial\langle z\rangle}{\partial z}.$$

- Substituting into Poisson's equation $\nabla\cdot\delta\mathbf{E}\simeq\partial\delta E_z/\partial z = 4\pi e_b\delta n$, we obtain the dispersion relation

$$1=\frac{\bar{\omega}_{pb}^2}{2}\left[\frac{1}{(\omega-\omega_{\beta\perp})^2}+\frac{1}{(\omega+\omega_{\beta\perp})^2}\right],$$

where $\bar{\omega}_{pb}^2 = 4\pi e_b^2 n_b/m_b$ is the beam plasma frequency squared.

Instability Mechanism (Growth rate)

- Using the definition of the depressed tune $\nu^2/\nu_0^2 = \omega_{\beta b}^2/\omega_f^2 = 1 - \bar{\omega}_{pb}^2/2\omega_f^2$ we can rewrite the dispersion relation as

$$\frac{\nu_n^2}{1-\nu_n^2} = \left[\frac{1}{(\omega_n/\nu_n - 1)^2} + \frac{1}{(\omega_n/\nu_n + 1)^2}\right],$$

  where $\nu_n = \nu/\nu_0$, and $\omega_n = \omega/\omega_f$.

- Solution of the dispersion equation is

$$\omega_n^2 = 1 \pm \sqrt{(1-\nu_n^2)(1+3\nu_n^2)}.$$

- The mode with lower sign in is unstable and purely growing for $\nu_n < \nu_n^{th} = \sqrt{2/3} \approx 0.82$.

- Maximum growth rate $(Im\omega)^{max}/\omega_f = \sqrt{2/\sqrt{3}-1} \approx 0.39$ occurs for $\nu_n^{max} = \sqrt{1/3} \approx 0.58$.

- $(Im\omega)/\omega_f \simeq \nu/\nu_0$ as $\nu/\nu_0 \to 0$.

BEST Nonlinear δF Simulation Code

- 3D particle-in-cell simulation code with cylindrical geometry.
- Multiple species.
- Adiabatic field pusher for light particles (electrons).
- Transition from delta-f to regular PIC code for large perturbations.
- Simulation noise is reduced significantly when operating as delta-f.
- Easily switched between linear and nonlinear operation.
- Written in Fortran 90/95 and extensively object-oriented.
- NetCDF data format for large-scale diagnostics and visualization.
- Achieved an average speed of 80 megaflops on IBM-SP (stage I) at NERSC.
- The code has been parallelized using OpenMP and MPI

BEST stands for "Beam Equilibrium, Stability and Transport code"

Description of the BEST Nonlinear δF Simulation Code

- Solution to the nonlinear Vlasov-Maxwell equations are expressed as

$$f_b = f_b^0 + \delta f_b, \quad \varphi = \varphi_0 + \delta\varphi, \quad A_z = A_z^0 + \delta A_z,$$

where $(f_b^0, \varphi^0, A_z^0)$ are known equilibrium solutions.

- Equations for the perturbed potentials are

$$\nabla^2 \delta\varphi = -4\pi e_b \int d^3 p \, \delta f_b, \qquad \nabla^2 \delta A_z = -\frac{4\pi}{c} e_b \int d^3 p \, \mathrm{v}_z \delta f_b,$$

$$\delta f_b = \sum_{i=1}^{N_{sb}} w_{bi} \delta(\vec{\mathrm{x}} - \vec{\mathrm{x}}_{\mathrm{bi}}) \delta(\vec{p} - \vec{p}_{bi}).$$

- Equation for the particle motion advance are

$$\frac{d\vec{x}_{bi}}{dt} = (\gamma_b m_b)^{-1} \vec{p}_{bi}, \qquad \frac{d\vec{p}_{bi}}{dt} = -\gamma_b m_b \omega_\perp^2 \vec{x}_{\perp bi} - e_b (\nabla\varphi - \frac{\mathrm{v}_{zbi}}{c} \nabla_\perp A_z),$$

$$\frac{dw_{bi}}{dt} = -(1 - w_{bi}) \frac{1}{f_{b0}} \frac{\partial f_{b0}}{\partial \vec{p}} \cdot \delta\left(\frac{d\vec{p}_{bi}}{dt}\right), \qquad \delta\left(\frac{d\vec{p}_{bi}}{dt}\right) = -e_b (\nabla \delta\varphi - \frac{\mathrm{v}_{zbi}}{c} \nabla_\perp \delta A_z).$$

Simulations show fast instability $\gamma \sim 0.1\omega_{pb}$

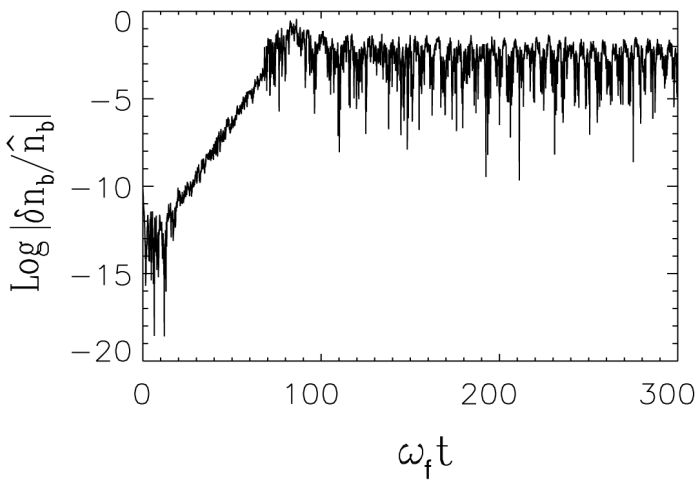

Parameters of the simulation:

$$T_{\|b} / T_{\perp b} = 0.01, \qquad r_w / r_b = 3,$$

where $r_b = \left\langle r^2 \right\rangle^{1/2}$.

Beam intensity parameter:

$$s_b = \hat{\omega}_{pb}^2 / 2\gamma_b^2 \omega_f^2 = 0.8$$

- Time history of density perturbation $\delta n_b = \int d^3 p \delta f_b$.

- The self-consistent equilibrium distribution functions is assumed to be:

$$f_b^0(r, p_\perp, p_z) = \frac{\hat{n}_b}{(2\pi\gamma_b m_b)^{3/2} \gamma_b T_{\perp b} T_{\|b}^{1/2}} \exp\left\{ -\frac{(p_z - \gamma_b m_b \beta_b c)^2}{2\gamma_b^3 m_b T_{\|b}} - \frac{p_\perp^2 / 2\gamma_b m_b + \gamma_b m_b \omega_f^2 r^2 / 2 + e_b(\varphi_0 - \beta_b A_{z0})}{T_{\perp b}} \right\}$$

Saturation of the instability

- The average longitudinal momentum distribution $F_b(p_z) = \int d^2 p_\perp d^3 x f_b$ for a dominant initial perturbation with m=1.

$$k_z r_w \approx 9.0, \quad s_b = 0.8.$$

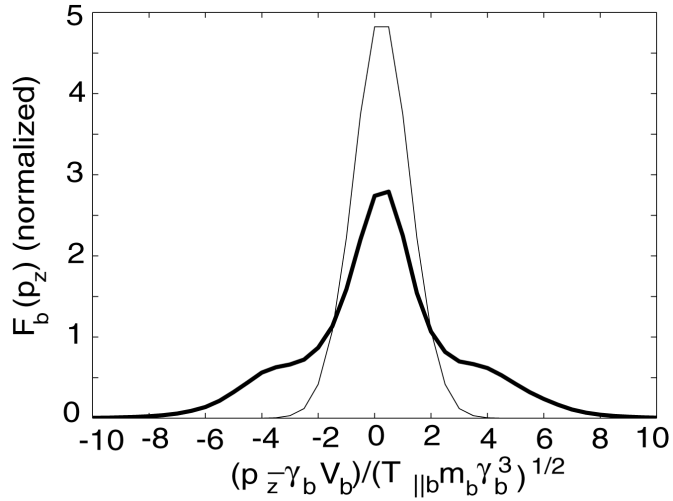

- Mode growth linearly with $\mathrm{Re}\,\omega = 0$.

- Mode saturates via particle trapping with consequent formation of tails in axial momentum space.

- The final width of the longitudinal velocity distribution can be estimated as $\Delta v_{||} \cong | v_{ph} - V_b |$, where $v_{ph} = \omega_{nl} / k_z$.

Grid Interaction and Artificial Heating in PIC codes

- Due to finite number of grid points the particle density with $k_p = k + p \cdot k_g$ will be represented by the same grid density $\rho \sim \sum \rho_j \exp(ik_p X_j) = \sum \rho_j \exp(ikX_j)$, where $k_g = 2\pi/\Delta z$ and $X_j = j \cdot \Delta z$.

- This will result in coupling of the main wave with wavenumber k with its aliases with wavenumbers $k_p = k + p \cdot k_g$, $\pm 1, \pm 2, \ldots$.

- The coupling strength A_p is smaller for smoother interpolation on the grid, e.i., smoother particle shape function $S(x)$: $A_p \sim |S(k_p)|^2$.

- The aliases can strongly interact with particles if $\omega/k_p \sim v_{th}^z$, or $\lambda_d^z \leq \Delta z$ (*Langdon, 1970*).

- Interaction will result in plasma heating until $\lambda_d^z \geq \Delta z$, when aliases stop growing due to the Landau damping.

- This artificial heating can be confused for the heating due to the temperature anisotropy instability.

Description of Beam Eigenmode And Spectra (bEASt) Code

- Code searches for the roots of the matrix dispersion relation.

- Electrostatic perturbations of the form

$$\delta\phi(\mathbf{x},t) = \widehat{\delta\phi}(r)\exp(im\theta + ik_z z - i\omega t)$$

  are assumed, where k_z is the axial wavenumber, m is the azimuthal mode number and ω is the complex oscillation frequency.

- Perturbations are about thermal equilibrium distribution in the beam frame($V_b = 0$)

$$f_b^0(r,\mathbf{p}) = \frac{\widehat{n}_b}{(2\pi m_b)^{3/2} T_{\perp b} T_{||b}^{1/2}} \exp\left(-\frac{H_\perp}{T_{\perp b}} - \frac{p_z^2}{2m_b T_{||b}}\right).$$

  Here, $H_\perp = p_\perp^2/2m_b + (1/2)m_b\omega_f^2(x^2+y^2) + e_b\phi^0(r)$ is the single-particle Hamiltonian for transverse particle motion, and $\omega_f = const.$ is the transverse focusing frequency.

Dispersion Matrix

- Perturbation is expanded into the complete set of vacuum eigenfunctions $\phi_n(r) = A_n J_m(\lambda_n r/r_w)$

$$\widehat{\delta\phi}(r) = \sum_n \alpha_n \phi_n(r),$$

where $J_m(\lambda_n) = 0$.

- Using the method of characteristics, analysis of the linearized Vlasov-Maxwell equations leads to an infinite dimension matrix dispersion equation

$$\sum \alpha_n D_{n,m}(\omega) = 0$$

- Dispersion matrix is

$$D_{n,n'}(\omega) = \frac{J_{m+1}^2(\lambda_n)}{2}(\lambda_n^2 + k_z^2 r_w^2)\delta_{n,n'} + \chi_{n,n'}(\omega),$$

where $\chi_{n,n'}$ is the beam-induced susceptibility.

Beam-Induced Susceptibility

- Beam-induced susceptibility is given by

$$\chi_{n,n'}(\omega) = \frac{r_w^2}{\lambda_d^2} q_{n,n'} + \int_0^\infty ds \exp\left(is\omega - \frac{s^2 k_z^2 T_{||}}{2m_b}\right) \times \left[i\omega + \left(1 - \frac{T_{||}}{T_\perp}\right)\frac{sk_z^2 T_\perp}{2m_b}\right] Q_{n,n'}(s),$$

where

$$Q_{n,n'}(s) = \frac{1}{m_b \lambda_d^2} \sum_p \int \frac{dP_\theta}{\omega_r} \frac{dH_\perp}{T_{\perp b}} \exp\left[-\frac{H_\perp}{T_{\perp b}}\right] (I_n^{p,m})^* I_{n'}^{p,m} e^{-is(p\omega_r + m\omega_\theta)}.$$

Here P_θ is the canonical angular momentum and $\lambda_d^2 = T_{\perp b}/4\pi e_b^2 \widehat{n}_b$ is the perpendicular Debye length-squared.

- $q_{n,n'}$ is defined by

$$q_{n,n'} = \int_0^1 dx x N(x) J_m(\lambda_n x) J_m(\lambda_{n'} x),$$

and the orbit integral is

$$I_n^{p,m}(H_\perp, P_\theta) = \int_0^{T_r} \frac{d\tau}{T_r} J_m\left[\frac{\lambda_n r(\tau)}{r_w}\right] e^{-ip\omega_r \tau + im[\theta(\tau) - \omega_\theta \tau]}$$

where $N(x) = n_b^0(x r_w)/\widehat{n}_b$ and $r(\tau)$ and $\theta(\tau)$ are the transverse orbits in the equilibrium field configuration.

Description of Beam Eigenmode And Spectra (bEASt) Code (continued)

The Beam Eigenmode and Spectra (bEASt) code solves the matrix dispersion equation in several steps:

- Particle orbits $r(\tau)$ and $\theta(\tau)$ in the equilibrium field configuration are calculated for one complete oscillation period T_r and the frequencies $\omega_r(H_\perp, P_\theta)$ and $\omega_\theta(H_\perp, P_\theta)$ are obtained.

- Fast fourier transform (FFT) is used to calculate the orbit integrals.

- Matrices $Q_{n,n'}(s)$ and $q_{n,n'}$ are calculated, stored, and then used repeatedly during the search for the eigenvector of the dispersion matrix $D_{n,n'}(\omega)$ with zero eigenvalue.

- Note that the matrices $Q_{n,n'}(s)$ and $q_{n,n'}$ are calculated only once, thanks to the separation of the particle variables $(H_\perp, P_\theta, r, \theta)$ from the dispersion equation variables ω and k_z.

Description of Beam Eigenmode And Spectra (bEASt) Code (continued)

- The typical number of particle trajectories used in the calculations is 300, with 16 time steps during one oscillation period T_r, which is significantly less than the number of particles and times steps used in PIC simulations.

- For moderately intense beams with $\nu/\nu_0 > 0.4$, the rank of the dispersion matrix $N = 6$ is sufficient for convergence of the results.

- As the beam intensity increases ($\nu/\nu_0 \rightarrow 0$) the eigenfunctions become localized at the beam edge and N increases sharply indicating the need for a different expansion basis.

- The method works well for finding the unstable modes, or slightly damped modes. For highly damped modes, an accurate integration requires calculation of the matrix $Q_{n,n'}(s)$ for values of $s > |Im\omega|/(k_z^2 T_\perp/m_b)$, which can be computationally extensive.

Numerical Results

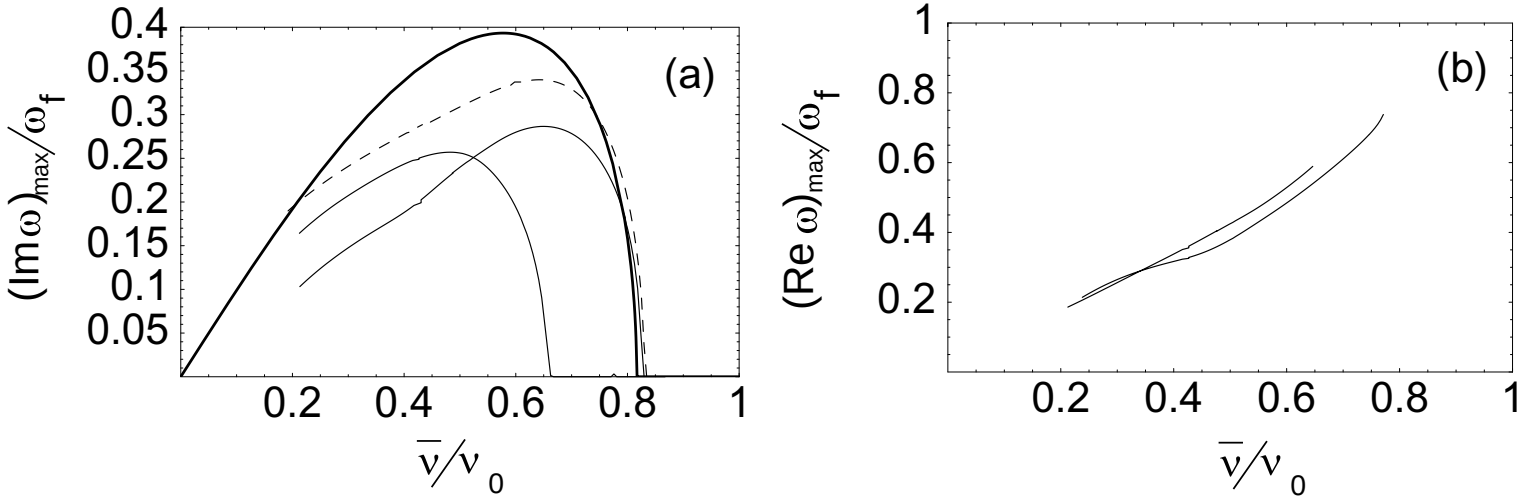

- Typical numerical results obtained using the bEASt code for the case where $r_w = 3r_b$, $T_{||b}/T_{\perp b} = 0$ and m=0 (solid curve) and m=1 (dotted curve). Thick solid curve corresponds to an approximate solution.

- The $m = 1$ dipole mode has the highest growth rate, $(Im\omega)/\omega_f \simeq 0.34$ and is purely growing, for $\bar{\nu}/\nu_0 \simeq 0.62$.

- The instability is absent for $\bar{\nu}/\nu_0 > 0.82$.

Numerical Results

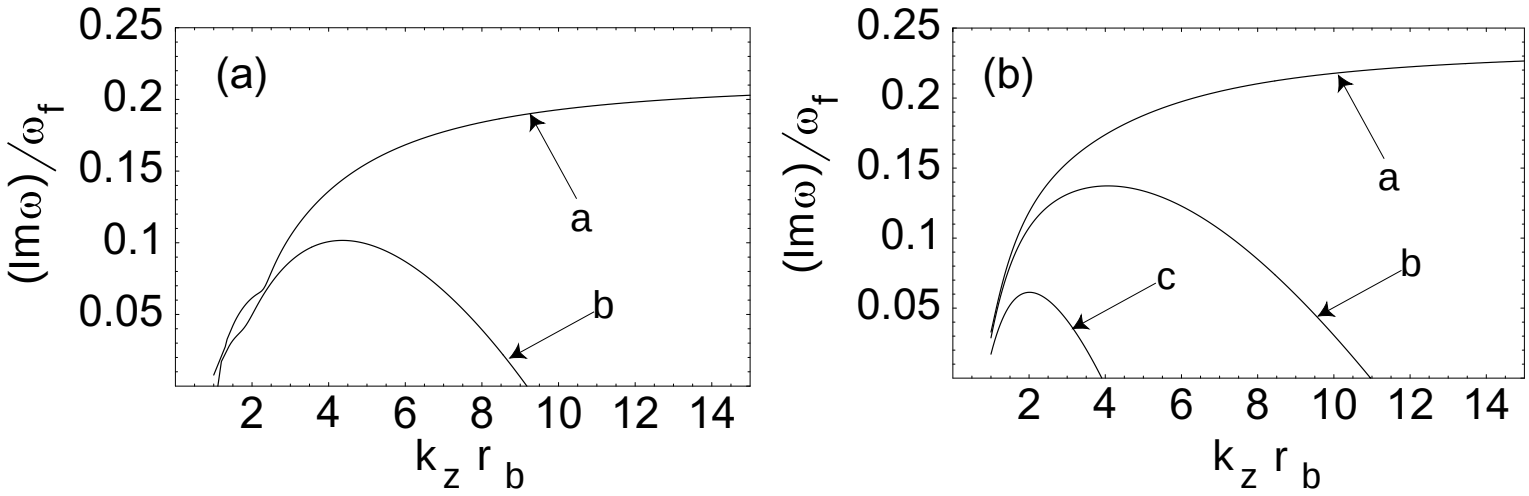

- $(Im\omega)/\omega_f$ versus $k_z r_b$ for $\bar{\nu}/\nu_0 = 0.3$ and several values of the temperature ratio $T_{||b}/T_{\perp b} = 0, 0.01, 0.05$(curves a,b and c). Here, figures (a) and (b) are for azimuthal mode number $m = 0$ and $m = 1$, respectively.

- Instability is present only for short-wavelength perturbations $k_z^2 r_b^2 > 1$.

- Finite $T_{||b}$ effects introduce a finite bandwidth in $k_z r_b$ for instability, since the modes with large values of $k_z r_b$ are stabilized by longitudinal Landau damping.

Numerical Results

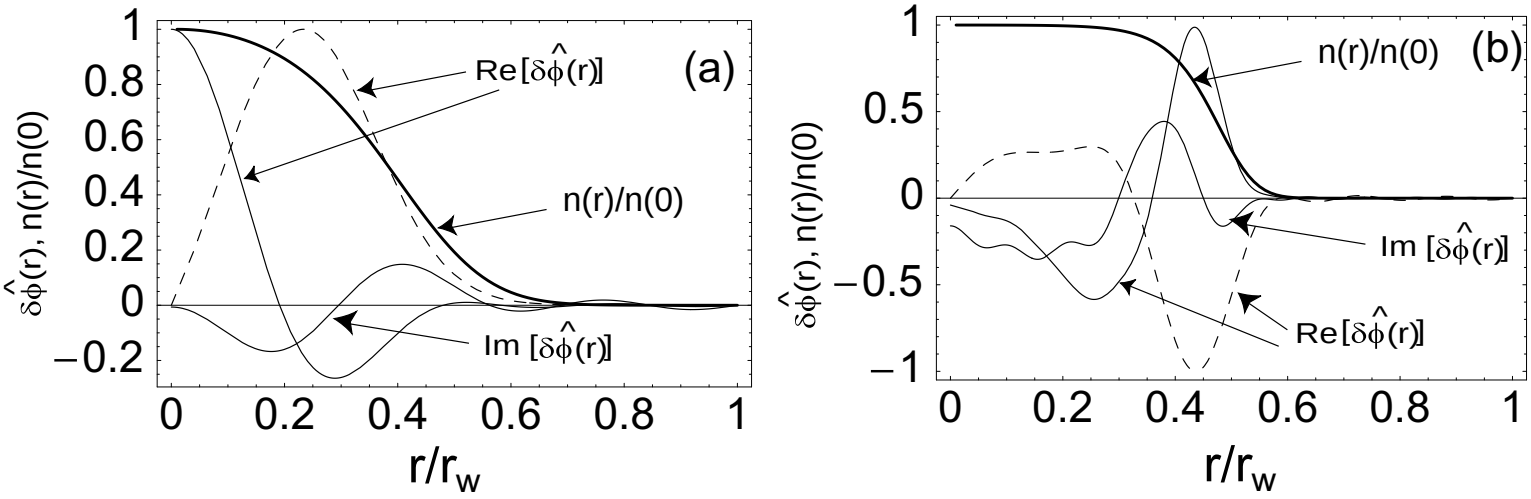

- Plots of the normalized eigenfunctions $Re[\delta\widehat{\phi}(r)]$ and $Im[\delta\widehat{\phi}(r)]$ for the most unstable modes versus r/r_w corresponding to m=0 (solid curves) and m=1 (dotted curve) and $\bar{\nu}/\nu_0 = 0.6$ (a) and $\bar{\nu}/\nu_0 = 0.3$ (b). Here, $T_{||b}/T_{\perp b} = 0$ and $k_z r_b = 20$.

- Thick solid curve corresponds to normalized density profile $n(r)/n(0)$.

- For smaller normalized depressed tune eigenfunctions become localized near the beam edge.

Numerical Results

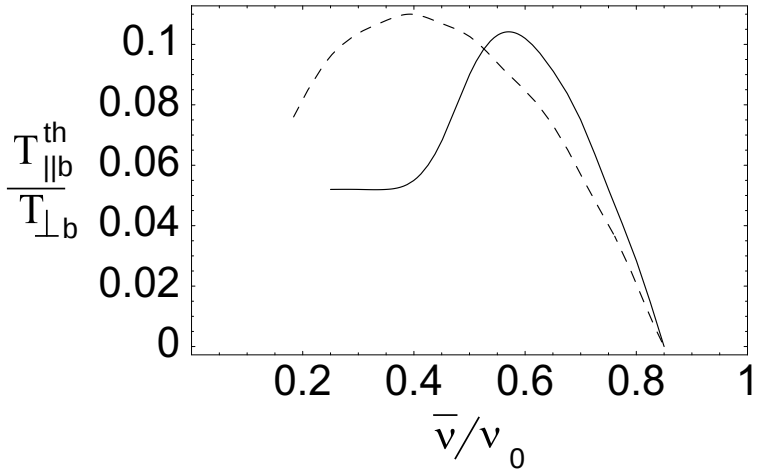

- Plots of the longitudinal threshold temperature $T^{th}_{||b}$ for the onset of instability normalized to the transverse temperature $T_{\perp b}$ versus normalized tune depression $\bar{\nu}/\nu_0$ for $m = 0$ (solid line) and $m = 1$ (dotted line).

- Due to accuracy limitations in the bEASt code, we define the threshold as the value of $T_{||b}/T_{\perp b}$ at which the maximum normalized growth rate becomes less then $(Im\omega)_{max}/\omega_f < 0.01$.

- Maximum threshold value, $T_{||b}/T_{\perp b} = 0.11$, is achieved for moderately intense beams with $\bar{\nu}/\nu_0 = 0.4$.

Conclusions

- bEASt code, which solves the matrix dispersion relation for electrostatic perturbations in intense particle beams, has been used to investigate the stability properties of intense charged particle beams with large temperature anisotropy ($T_{||b}/T_{\perp b} \ll 1$) over a wide range of normalized tune depression, $0.2 < \bar{\nu}/\nu_0 < 1$.

- The numerical results clearly show that intense beams with $\bar{\nu}/\nu_0 < 0.82$ are linearly unstable to short-wavelength perturbations with $k_z^2 r_b^2 \geq 1$.

- The instability is kinetic and is due to the coupling of the particles transverse betatron motion with the longitudinal plasma oscillations excited by the perturbation.

- The most unstable mode is found to be a purely growing dipole mode with normalized growth rate $Im\omega/\omega_f \simeq 0.34$ for $\bar{\nu}/\nu_0 \simeq 0.62$ and $T_{||b}/T_{\perp b} = 0$.

- The growth rate is proportional to the normalized tune $Im\omega/\omega_f \approx \bar{\nu}/\nu_0$ for $\bar{\nu}/\nu_0 \ll 1$.

- The instability is stabilized by longitudinal Landau damping whenever the ratio of the longitudinal and transverse temperatures satisfies $T_{||b}/T_{\perp b} > 0.11$.